Circulation Journal
Circ J 2021; 85: 1806–1813
doi:10.1253/circj.CJ-20-0862

Polarimetric Signatures of Coronary Thrombus in Patients With Acute Coronary Syndrome

Laurens J. C. van Zandvoort, PhD; Kenichiro Otsuka, MD, PhD; Martin Villiger, PhD; Tara Neleman, BSc; Jouke Dijkstra, PhD, BSc; Felix Zijlstra, MD, PhD; Nicolas M. van Mieghem, MD, PhD; Brett E. Bouma, PhD; Joost Daemen, MD, PhD

Background: Intravascular polarization-sensitive optical frequency domain imaging (PS-OFDI) offers a novel approach to measure tissue birefringence, which is elevated in collagen and smooth muscle cells, that in turn plays a critical role in healing coronary thrombus (HCT). This study aimed to quantitatively assess polarization properties of coronary fresh and organizing thrombus with PS-OFDI in patients with acute coronary syndrome (ACS).

Methods and Results: The POLARIS-I prospective registry enrolled 32 patients with ACS. Pre-procedural PS-OFDI pullbacks using conventional imaging catheters revealed 26 thrombus-regions in 21 patients. Thrombus was manually delineated in conventional OFDI cross-sections separated by 0.5 mm and categorized into fresh thrombus caused by plaque rupture, stent thrombosis, or erosion in 18 thrombus-regions (182 frames) or into HCT for 8 thrombus-regions (141 frames). Birefringence of coronary thrombus was compared between the 2 categories. Birefringence in HCTs was significantly higher than in fresh thrombus (Δn=0.47 (0.37–0.72) vs. Δn=0.25 (0.17–0.29), P=0.007). In a subgroup analysis, when only using thrombus-regions from culprit lesions, ischemic time was a significant predictor for birefringence (ß (Δn)=0.001 per hour, 95% CI [0.0002–0.002], P=0.023).

Conclusions: Intravascular PS-OFDI offers the opportunity to quantitatively assess the polarimetric properties of fresh and organizing coronary thrombus, providing new insights into vascular healing and plaque stability.

Key Words: Birefringence; Optical coherence tomography; Polarimetry; Polarization-sensitive; Thrombus

Acute coronary syndrome (ACS) is a life-threatening coronary thrombotic complication,[1] caused by plaque rupture (PR), plaque erosion, calcified nodules, or stent-related issues.[2–5] Although coronary thrombosis may precipitate ACS, it is well understood that subclinical coronary thrombus formation and its organizing process are common in the progression of chronic coronary artery disease.[6] Therefore, assessing the organization of coronary thrombus is important to understand the vascular healing process in patients.

Histopathological studies identified 3 stages in the evolution of coronary thrombus.[7–9] First, fresh thrombus (<1 day) is formed, comprising platelet aggregates, erythrocytes, intact granulocytes, and fibrin. Second, evolution into lytic thrombus (1–5 days) is characterized by the appearance of necrotic areas and granulocytes. Third, organized thrombus (>5 days) is hallmarked by the presence of smooth muscle cells (SMCs), homogeneous or hyaline fibrin, deposition of connective tissue, and capillary vessel ingrowth.

Intravascular optical coherence tomography (OCT) permits accurate identification of fresh coronary thrombus and differentiation between erythrocyte-rich 'red' thrombus and predominantly platelet-containing 'white' thrombus.[10–12] Although OCT has been reported to be able to identify newer intima that covers healing or healed coronary plaques by its appearance of smooth layered structures, this relies on subjective and qualitative image interpretation, without insight into the underlying tissue morphology of composition.[13] The conventional OCT signal is insensitive to the composition and the age of fresh or healing coronary thrombus (HCT).

Pioneering research by Villiger et al and Otsuka et al demonstrated the ability of intravascular polarimetry with

Received September 1, 2020; revised manuscript received December 17, 2020; accepted February 19, 2021; J-STAGE Advance Publication released online April 7, 2021 Time for primary review: 28 days

Department of Cardiology, Thoraxcenter, Erasmus University Medical Center, Rotterdam (L.J.C.v.Z., T.N., F.Z., N.M.v.M., B.E.B., J. Daemen), The Netherlands; Wellman Center for Photomedicine, Massachusetts General Hospital, Harvard Medical School, Boston, MA (K.O., M.V., B.E.B.), USA; Division of Image Processing, Department of Radiology, Leiden University Medical Center, Leiden (J. Dijkstra), The Netherlands; and Institute for Medical Engineering and Science, Massachusetts Institute of Technology, Cambridge, MA (B.E.B.), USA

Mailing address: Joost Daemen, MD, PhD, Department of Cardiology, Room Rg-628, Erasmus University Medical Center, P.O. Box 2040, 3000 CA Rotterdam, The Netherlands. E-mail: j.daemen@erasmusmc.nl

ISSN-1346-9843

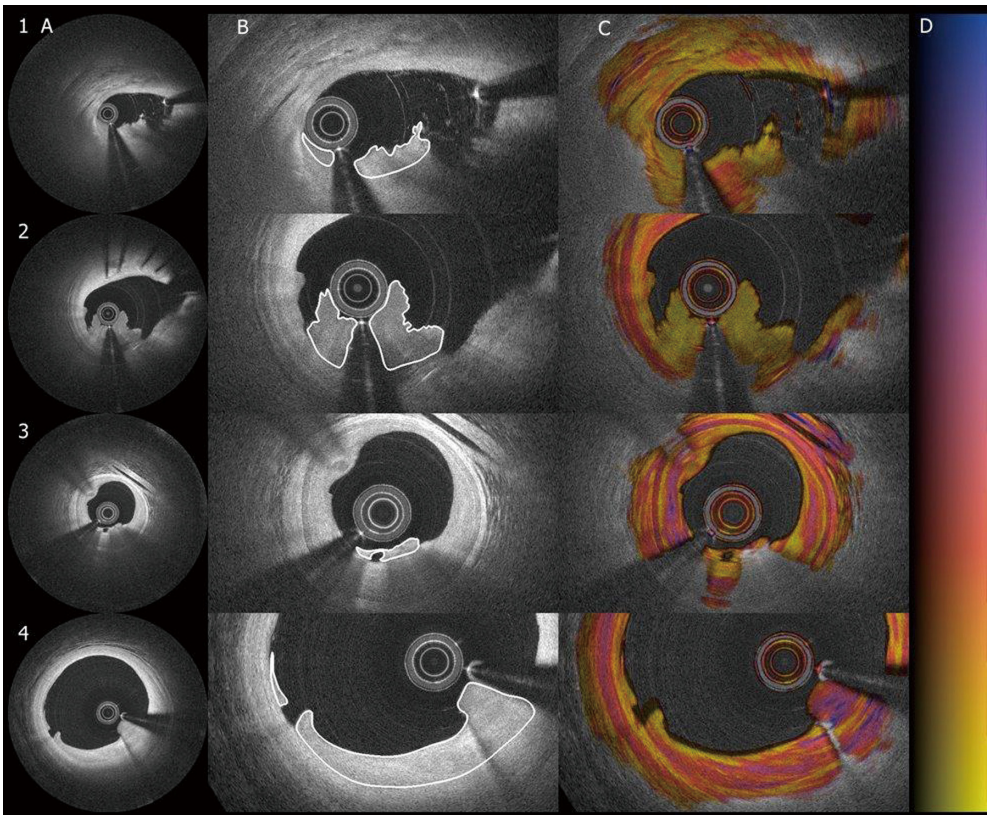

Figure 1. Delineation of four types of thrombi in intensity and birefringence images. Four different categories of coronary thrombi, panel 1 through 3, are fresh thrombi. **1**, plaque rupture; **2**, stent thrombosis; **3**, erosion; **4**, healing coronary thrombus. (**A**) Standard intensity image; (**B**) magnified in the intensity images with thrombus delineation; (**C**) corresponding birefringence images; (**D**) color grading of the polarization signal.

polarization-sensitive (PS) optical frequency domain imaging (OFDI) to quantitatively measure birefringence and depolarization. These intrinsic tissue properties serve as an endogenous contrast mechanism and enabled differentiating between morphometric plaque properties.[14,15] In particular, collagen and SMCs have been shown to display increased birefringence due to their fibrillary architecture.[14,16] Because these components play a pivotal role in the evolution of thrombus, we aimed to investigate the polarimetric properties of thrombus-containing regions in patients with ACS and to explore their association with clinical parameters.

Methods

Study Population

Patients were included as part of the POLARIS-I prospective registry. This single center registry enrolled patients presenting with ACS (being either unstable angina, non-ST segment elevation myocardial infarction or ST segment elevation myocardial infarction) with an indication to perform intravascular imaging using conventional OFDI. Patients presenting with cardiogenic shock or severe hemodynamic instability were excluded. Additionally, patients with a known allergy to contrast media, severe impaired renal function (estimated glomerular filtration rate $<35\,mL/min/1.73\,m^2$), or other reasons impeding OFDI imaging were also excluded.

PS-OFDI Image Acquisition

PS-OFDI acquisition was performed with commercialized OFDI catheters and the matching pullback device (FastView, Terumo Corporation) interfaced with a custom-built state-of-the-art PS-OFDI console.[14] Pullbacks were performed at pullback speeds of 10 or 20 mm/s at the operator's discretion. Conventional OFDI intensity images were used in the catheterization laboratory to provide the operator with ad-hoc information on the coronary anatomy and the location of interest. Reconstruction of the polarimetric signals was performed offline (reconstruction is sufficiently fast to permit integration into the catheterization laboratory workflow if ad-hoc polarization properties are required in future studies). No complications due to PS-OFDI imaging were encountered. The study was performed in accordance with the Declaration of Helsinki. The study protocol was approved by the local ethics committee on May 8 2018 (study ID: MEC-2018-1193). Patients provided written informed consent for the procedure and we used anonymous datasets for research purposes in alignment with the Dutch Medical Research Act.

Study Definitions

Culprit lesions were defined as the leading cause for the experienced ACS and comprised the most severe narrow-

ing of the coronary lumen, as appreciated in the OFDI intensity images.

Ischemic time was defined as the time between the onset of acute symptoms and the start of the percutaneous coronary intervention (PCI). In the absence of abrupt symptoms, the time to first detect elevated high-sensitivity cardiac troponin was taken as the onset. The ischemic time served as an estimate for the age of thrombus, only if thrombi were located in the culprit lesion.

Conventional OFDI Delineation and Analysis

Thrombus-regions were defined as adjacent frames containing visible thrombus in the conventional OFDI intensity images. Multiple thrombus-regions could be present within a pullback. Thrombus-regions were categorized into one of 4 groups based on their appearance in the intensity images: thrombus due to PR, stent thrombosis (ST), thrombus due to plaque erosion and finally thrombus in the form of HCT (**Figure 1**).[17] Thrombus was allocated to the PR group if a rupture site could be visualized. Thrombus attached to a previously implanted stent was allocated to the ST group. Irregularly shaped thrombus in a non-lipid rich region without evident signs of rupture was labelled as plaque erosion. Finally, HCTs were defined as smooth layered structures located flat against the luminal wall without any current sign of rupture.[13] For statistical analysis, HCTs were compared to fresh thrombus, compounding PR, ST and plaque erosions.

Volumetric luminal analysis of the thrombus-region was performed in fixed 0.5 mm frame-intervals using QCU-CMS viewing software (Leiden University Medical Centre, Leiden, The Netherlands). Manual lumen and thrombus segmentation in the corresponding frames was performed using a dedicated user interface written in MATLAB (The MathWorks, Inc., Natick, MA, USA). High attenuating thrombus was merely delineated to the extent that the backscattering signal allowed for accurate thrombus identification (**Figure 1**). Segmentation was performed independently by 2 OCT/OFDI experts (L.J.C.v.Z., K.O.), followed by a consensus meeting. Volume analysis was performed using the disk summation method. Additional analysis was performed at the shoulder of identified plaque ruptures, in the first frame with an intact fibrous cap, either distal or proximal to the plaque rupture, and in additional cross-sections of remote fibroatheromas. The intact fibrous caps overlying highly attenuating lipid-rich plaque were manually delineated. Minimum fibrous cap thickness and fibrous cap area were measured with the dedicated MATLAB interface.

Polarimetry Analysis

Analysis of birefringence and depolarization was performed at Massachusetts General Hospital (Boston, MA, USA) where the conventional OFDI analysis and clinical information from the patients at the Erasmus Medical Center (Rotterdam, The Netherlands) was blinded. Polarimetric measurements were automatically computed based on the segmentation in the conventional OFDI images. Birefringence (Δn) describes the difference of the refractive indices experienced by light polarized parallel and orthogonal to the fibrillary tissue components.[18] Median values, β's and 95% confidence interval (CI) for birefringence are given in units of 10^{-3} throughout this manuscript.

Depolarization is related to the randomization of the detected polarization states within a small region around each pixel. It is expressed as the ratio of the depolarized signal divided by the total signal.[18] Depolarization ranges from 0 to approximately 0.5; however, above 0.2, the increased randomization of the polarization states makes accurate evaluation of birefringence difficult.[18] Therefore, in the current study, median birefringence measurements were only assessed in regions with a depolarization ≤ 0.2.

Statistical Analysis

Categorical variables are reported as counts (percentage) and continuous variables are reported as mean±standard deviation (SD) or median±interquartile range (IQR). Variables were compared using a generalized linear mixed-effects model (GLME-model) with a random effect for the patient. The GLME-model was conducted to correct for the possible presence of multiple thrombi in a single patient. On a frame level, variables were compared using a nested GLME model, with a random effect for frames in each thrombus-region nested within each vessel. Subsequently, using a median Δn as the independent variable, any univariate predictor with a $P<0.05$ was inserted into a multivariate (nested) GLME model. Δn distributions were calculated by counting the relative occurrence of Δn values within 52 equally spaced bins in the range from 0 to 2.0×10^{-3} across all frames of each thrombus-region. Distribution plots report the mean values±SD of each bin across all thrombus-regions within either of the HCT or the fresh thrombus groups. All tests were 2-tailed and a $P<0.05$ was considered statistically significant. All statistical analyses were performed using R (version 3.5.1, packages: lme4).

Results

Baseline Patient Characteristics

The Polaris-I registry included 32 patients (38 vessels) undergoing pre-PCI PS-OFDI. Pullbacks in 5 patients could not be used for the current analysis due to insufficient flushing with contrast medium (n=3), catheter malfunction (n=1), or failure to assess the polarization states (n=1). From the remaining 27 patients with suitable OFDI acquisition, 21 patients (21 vessels) displayed ≥1 coronary thrombi when conventional OFDI pullbacks were used. **Table 1** shows the baseline characteristics of all patients with coronary thrombus identified in the OFDI intensity images. Patients with coronary thrombus were of male gender (62%), had diabetes mellitus (29%), and presented with unstable angina and non-ST segment myocardial infarction (14% and 76%, respectively). All patients were preloaded with aspirin and P2Y12 inhibitors at the time of diagnosis.

Thrombus Characteristics

A total of 26 thrombus-regions were identified, and grouped as 15 PR, 2 ST, 1 plaque erosion and 8 HCT. No fresh thrombi in lipid rich plaques without signs of rupture were found. The thrombus-region was within the culprit lesion in 17 cases (65 %) (**Table 2**). HCTs were less often located within the culprit lesion as compared to fresh thrombus (25% vs. 83%, P=0.004). For patients with thrombus-containing culprit lesions, the median time between onset of symptoms and intravascular imaging was 27 (14.5–86) h. The 26 thrombus-regions comprised a total of 1,666 frames with thrombus. At an interval of 0.5 mm, 323 frames were subsequently analyzed; 160 frames

belonging to PR, 16 to ST, 6 to plaque erosion and 141 to HCT (**Table 3**). The median birefringence and depolarization of all thrombus-regions were 0.28 (0.21–0.45) and 0.07 (0.05–0.08), respectively.

Polarimetric Analysis of Thrombus

In the univariate GLME analysis, on a thrombus-region level, HCTs displayed significantly higher birefringence than fresh thrombus (Δn=0.47 (0.37–0.72) vs. Δn=0.25 (0.17–0.29), P=0.007) (**Table 2**). The birefringence did not differ between the types of fresh thrombi. In an unadjusted subgroup analysis (**Table 4**), only using thrombus-regions from culprit lesions, for which ischemic time can serve as a metric of thrombus age, the ischemic time was a significant predictor for birefringence (ß (Δn)=0.001 per hour, 95% CI [0.0002–0.002], P=0.023). **Figure 2** shows the distribution of birefringence found in fresh thrombi and HCTs, respectively.

The univariate GLME model on a frame level demonstrates predictors for birefringence (**Table 5**). First, the type of thrombus, specifically HCT, was a significant predictor for birefringence (ß (Δn)=0.27, 95% CI [0.13–0.42], P=0.006). Additionally, thrombi in culprit lesions displayed lower birefringence (ß (Δn)=−0.17, 95% CI [−0.31 to −0.04], P=0.015). Finally, the ischemic time was significantly correlated to birefringence (ß (Δn)=0.001 per hour, 95% CI [0.00002–0.0021], P=0.022). In a multivariate GLME model on a frame level, including the effect of HCT and whether the thrombus was located at the culprit site, only HCT was a predictor for birefringence (ß (Δn)=0.26, 95% CI [0.12–0.39], P<0.001). No difference in depolarization was observed between the thrombus types on a lesion or frame level.

Polarimetric Analysis of Fibrous Caps

A total of 18 fibrous caps were analysed; 9 from the shoulders of ruptured plaques, and 9 from remotely located fibroatheromas. The median cap thickness did not differ between the ruptured and non-ruptured caps (108 μm (97–142) vs. 121 μm (109–163) respectively, P=0.258) (**Table 6**). Birefringence and depolarization measurements displayed similar values between the groups.

Table 1. Baseline Patient Characteristics

Variable	Patients with confirmed thrombus, confirmed with OFDI (n=21)
Gender (male)	13 (62)
Age (years)	65.3±13.3
Hypertension	16 (76)
Hypercholesterolemia	10 (48)
Diabetes mellitus	6 (29)
Family history of CAD	9 (43)
Smoking history	12 (57)
Prior myocardial infarction	6 (29)
Prior PCI	8 (38)
Prior target vessel PCI	5 (24)
Prior CABG	1 (5)
Indication for PCI	
Unstable angina	3 (14)
NSTEMI	16 (76)
STEMI	2 (10)
>1 vessel treated	6 (29)
Culprit vessel	
LAD	8 (38)
LCX	6 (29)
RCA	7 (33)
Cardiac enzymes at time of presentation	
hs-cTn T (ng/L)	178 (47~953)
hs-cTn I (ng/L)	65 (11~538)
CK	97 (63~339)
CK-MB	33 (3~59)
Ischemic time (h)	34 (17~91)
LDL-cholesterol mg/dL	3.51 (2.37~3.77)
Hematocrit	0.40 (0.36~0.43)
Antithrombotic therapy before presentation	
NOAC	3 (14)
ASA	5 (24)
P2Y12 inhibitor	4 (19)
Antithrombotic loading strategy at time of ACS	
ASA	21 (100)
Clopidogrel	6 (29)
Prasugrel	0 (0)
Ticagrelor	15 (71)
Glycoprotein IIb/IIIa inhibitors	0 (0)

Data are presented as mean±SD, median (IQR) or n (%). ACS, acute coronary syndrome; ASA, acetylsalicylic acid; CABG, coronary artery bypass graft; CAD, coronary artery disease; CK, creatine kinase; hs-cTn, high-sensitivity cardiac troponin; LAD, left anterior descending artery; LCX, left circumflex artery; LDL, low-density lipoprotein; NOAC, novel oral anticoagulants; NSTEMI, non-ST segment elevation myocardial infarction; OFDI, optical frequency domain imaging; PCI, percutaneous coronary intervention; RCA, right coronary artery; STEMI, ST segment elevation myocardial infarction.

Discussion

The POLARIS-I registry was designed to investigate the polarization signatures of coronary thrombus with intravascular polarimetry in patients with ACS. We demonstrate, for the first time, a significantly higher birefringence in HCTs than in fresh thrombus. Additionally, we found that birefringence of coronary thrombus increased with extending ischemic time, which is likely indicative of thrombus age. Finally, we observed no difference in birefringence between fibrous caps of ruptured plaques and those of remote fibroatheromas within the present cohort of patients with ACS.

OCT modalities currently provide the highest spatial resolution for intravascular imaging, providing the operator with an in-depth evaluation of the coronary wall in an acute setting.[19,20] Conventional OCT can differentiate between red and white thrombus based on their signal attenuation and this helps to identify the lesion morphology underlying an ACS. Pathological research indicated that a PR can occur silently, without causing physical symptoms, and that these thrombotic regions subsequently start to heal.[21] There remains a clear need to better understand the evolution and possible impairment of vascular healing, initiated by thrombus formation and its subsequent organization.[10–12] Yet, to date, thrombus age and composition can only be reliably assessed using histopath-

Table 2. Thrombus Characteristics on a Thrombus-Region Level

Variable	Plaque rupture (n=15)	Stent thrombosis (n=2)	Plaque erosion (n=1)	Fresh thrombus§ (n=18)	Healing coronary thrombus (n=8)	P value†
Culprit lesion	13 (87)	2 (100)	0 (0)	15 (83)	2 (25)	0.004
Ischemic time (h)‡	24 (15~57)	49 (2~)	–	24 (12~65)	169 (144~)	0.0001
Mean lumen area	2.80 (1.91~4.40)	6.34 (6.00~)	2.01	3.24 (1.98~5.16)	5.53 (3.00~7.41)	0.068
Minimum lumen area	1.31 (0.99~2.57)	4.96 (4.74~)	1.55	1.84 (1.04~3.08)	3.36 (1.89~6.32)	0.095
Maximum lumen area	4.52 (3.03~7.47)	7.59 (5.51~)	2.60	4.83 (3.00~7.52)	8.03 (4.24~12.86)	0.055
Thrombus volume (mm^3)	1.59 (1.05~3.20)	1.74 (1.21~)	0.22	1.48 (0.90~2.59)	2.8 (2.06~13.59)	0.074
Birefringence (Δn)	0.26 (0.17~0.31)	0.16 (0.12~)	0.25	0.25 (0.17~0.29)	0.47 (0.37~0.72)	0.007
Birefringence (Δn) staging						
<0.25	7 (47)	2 (100)	0 (0)	9 (50)	0 (0)	0.023
0.25~0.40	7 (47)	0 (0)	1 (100)	8 (44)	2 (25)	0.420
>0.40	1 (6)	0 (0)	0 (0)	1 (6)	6 (75)	0.001
Depolarization	0.06 (0.05~0.08)	0.16 (~0.28)	0.20	0.06 (0.05~0.12)	0.07 (0.05~0.08)	0.337

Data are presented as median (IQR) or n (%). †Fresh thrombus as compared to healing coronary thrombus. ‡Only for thrombus-regions located in culprit lesions. §Fresh thrombus is comprised of plaque ruptures, erosions and stent thrombosis.

Table 3. Thrombus Characteristics on a Frame Level

Variable	Plaque rupture (n=160)	Stent thrombosis (n=16)	Plaque erosion (n=6)	Fresh thrombus‡ (n=182)	Healing coronary thrombus (n=141)	P value†
Culprit lesion	149 (93)	16 (100)	0 (0)	165 (91)	33 (23)	<0.001
Lumen area (mm^2)	2.80 (1.75~4.46)	6.17 (5.55~7.26)	1.93 (1.70~2.36)	2.89 (1.83~5.19)	5.34 (3.40~10.55)	0.069
Mean lumen diameter (mm)	1.89 (1.49~2.38)	2.80 (2.66~3.04)	1.57 (1.47~1.73)	1.92 (1.53~2.57)	2.61 (2.08~3.67)	0.068
Minimum lumen diameter (mm)	1.39 (1.07~1.94)	1.95 (1.68~2.32)	1.41 (1.34~1.61)	1.45 (1.11~1.95)	2.22 (1.84~3.02)	0.028
Maximum lumen diameter (mm)	2.34 (1.87~3.06)	3.48 (3.25~3.56)	1.73 (1.62~1.87)	2.39 (1.87~3.18)	2.97 (2.20~4.17)	0.092
Thrombus area (mm^2)	0.39 (0.18~0.58)	0.48 (0.15~0.62)	0.07 (0.03~0.11)	0.38 (0.17~0.58)	0.61 (0.33~0.95)	0.070
Birefringence (Δn)	0.22 (0.15~0.30)	0.14 (0.12~0.19)	0.25 (0.22~0.28)	0.22 (0.14~0.29)	0.45 (0.38~0.59)	0.006
Depolarization	0.06 (0.05~0.09)	0.05 (0.03~0.23)	0.20 (0.15~0.23)	0.06 (0.05~0.09)	0.07 (0.05~0.09)	0.330
Ischemic time (h)*	24 (18~39)	96 (2~96)	–	24 (17~49)	195 (169~195)	0.118

Data are presented as median (interquartile range) or n (%). *Ischemic time is only available in the subgroup of culprit lesions. †Fresh thrombus as compared to healing coronary thrombus. ‡Fresh thrombus is comprised of plaque ruptures, erosions and stent thrombosis.

Table 4. Unadjusted Predictors for Birefringence on a Thrombus-Region Level

	β	P value	95% CI
Healing coronary thrombus	0.28	0.007	0.13~0.44
Culprit lesion	−0.17	0.061	−0.36~0.01
Lumen area (mm^2)	0.02	0.194	−0.01~0.05
Minimum lumen area (mm^2)	0.03	0.114	−0.01~0.07
Maximum lumen area (mm^2)	0.01	0.317	−0.01~0.03
Thrombus volume (mm^3)	0.00004	0.601	−0.00002~0.00002
Ischemic time (h)†	0.001	0.023	0.0002~0.002

†Ischemic time is only available in the subgroup of culprit lesions. CI, confidence interval.

ological examination, which has no place in an acute setting.[8]

Intravascular polarimetry with PS-OFDI is an extension of the conventional OCT that enables accurate measurement of the birefringence induced by organized linear structures such as SMCs and collagen.[14,22] The latter is illustrated by the high birefringence of the tunica media, which is rich in tightly arrayed SMCs.[14] Birefringence and polarization data should be seen as complimentary to the standard structural intensity signal and may provide more detailed information on the composition, and, hence, stability of the underlying plaque. In a previous study of intravascular polarimetry, we observed low birefringence in white thrombus but did not investigate HCTs.[14,15] In the current study, HCTs displayed significantly higher birefringence than fresh thrombus. Fresh thrombus is primarily unorganized whereas in a later stage, linear fibrillar structures such as connective tissue and SMCs emerge, which are absent immediately after an acute coronary event.[7–9] This SMC proliferation and collagen synthesis can explain the observed increase in birefringence.

Furthermore, we demonstrated that location of the thrombus remote from the culprit site and ischemic time were univariate predictors of birefringence. It should be

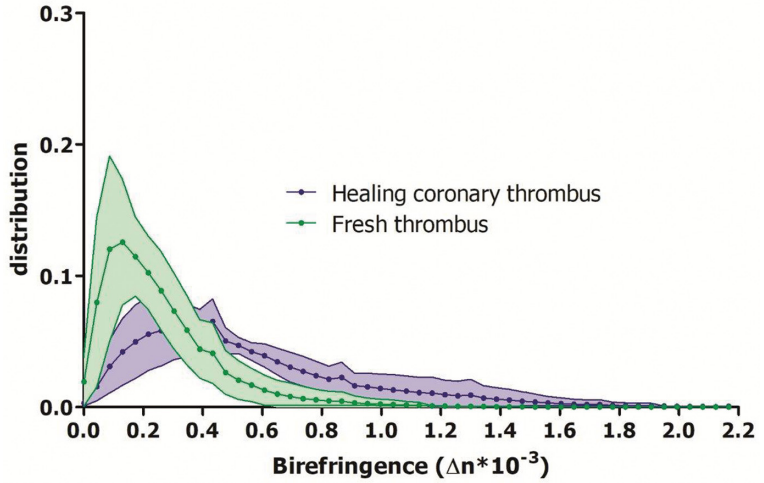

Figure 2. Birefringence distribution of healing coronary thrombus (HCT) and fresh thrombus. Purple and green lines indicate the relative frequency of a given birefringence value of HCT and fresh thrombus, respectively, averaged across all thrombus-regions of each group. The shaded areas indicate the standard-deviation across the thrombus-regions. Birefringence of HCT is higher than that of fresh thrombus.

Table 5. Unadjusted and Adjusted Predictors for Birefringence on a Frame Level

	Unadjusted			Adjusted		
	β	P value	95% CI	β	P value	95% CI
Healing coronary thrombus	0.27	0.006	0.13~0.42	0.26	<0.001	0.12~0.39
Plaque rupture	−0.17	0.051	−0.35~0.0001	–	–	–
Stent thrombosis	−0.19	0.212	−0.54~0.16	–	–	–
Plaque erosion	−0.09	0.648	−0.61~0.43	–	–	–
Culprit lesion	−0.17	0.015	−0.31~−0.04	−0.03	0.660	−0.16~0.10
Lumen area (mm^2)	−0.003	0.380	−0.009~0.003	–	–	–
Mean lumen diameter (mm)	−0.003	0.818	−0.03~0.02	–	–	–
Minimum lumen diameter (mm)	0.01	0.309	−0.01~0.04	–	–	–
Maximum lumen diameter (mm)	−0.02	0.155	−0.04~0.006	–	–	–
Thrombus area (mm^2)	0.000002	0.908	−0.00003~0.00004	–	–	–
Ischemic time (h)†	0.001	0.022	0.00002~0.002	–	–	–

†Ischemic time is only available in the subgroup of culprit lesions, and hence cannot be included independently in the adjusted model.

Table 6. Birefringence in the Caps at the Shoulder of Plaque Ruptures and Remote Fibroatheromas

Variable	Cap at shoulder of plaque rupture (n=9)	Cap of intact remote fibroatheroma (n=9)	P value
Minimal fibrous cap thickness (μm)	108 (97~142)	121 (109~163)	0.258
Fibrous cap area (mm^2)	0.12 (−0.07~031)	0.31 (0.15~0.45)	0.161
Birefringence (Δn)	0.29 (0.22~0.36)	0.29 (0.23~0.36)	1.000
Depolarization	0.11 (0.09~0.15)	0.09 (0.08~0.13)	0.340

Data are presented as median (interquartile range).

taken into account, however, that the ischemic time is highly correlated to the thrombus type, as can be appreciated in **Table 2**. It is plausible that impaired vascular healing after silent PR or plaque erosion leads to symptomatic ACS, but this phenotype would be challenging to diagnose with conventional OCT/OFDI. Indeed, plaques with a layered appearance in the OCT intensity signal have been shown to exhibit histopathological features of newer intima covering the original lesion substrate as a result of vascular healing, without, however, offering insight into its temporal course. Our observations suggest that PS-OFDI offers unique insight into the vascular healing process through the signatures that the thrombus organization imparts on the polarization of the near infrared light used for OCT/OFDI.[13]

Previous research hypothesized that fibrous caps that are prone to rupture would display lower birefringence compared to stable caps due to a lack of collagen that impairs mechanical stability.[23] In our sub-analysis comparing fibrous caps at the shoulder of ruptured plaques with caps of remote non-ruptured fibroatheromas in a limited number of patients with ACS, no difference was observed

in birefringence or cap thickness. The thickness of the cap, measured just proximal or distal of the rupture, is probably not representative of the thickness of a fibrous cap that is prone to rupture in the near future. With the current analysis, we aimed to provide detail on the cap integrity by assessing additional biomechanical factors related to plaque structural stress on top of conventional thickness measurements.[24] Furthermore, median birefringence in both ruptured caps and the caps of remote lesions were relatively low compared to the birefringence measured in fibrous plaques, suggesting a lower collagen content in ACS caps than in evidently fibrous plaques.[15] This may be explained by increased collagenolytic activity of inflammation within the entire culprit arteries in patients with ACS.[2,15]

Affect on Daily Practice

Coronary thrombus formation and its organizing process following subclinical PR play a pivotal role in disease progression. Birefringence, measured with PS optical frequency domain imaging (PS-OFDI), provides unique insights into the tissue composition of organizing coronary thrombus. In the present study, we demonstrated for the first time that birefringence of healing thrombus was significantly higher than that of fresh thrombus; our observations suggest that assessing composition of coronary thrombus with PS-OFDI offers a novel approach for studying vascular healing and plaque vulnerability in patients. Therefore, birefringence could provide clinicians with quantitative data on the biomechanical integrity of thrombus, providing a more personalized approach to treatment strategies.

Study Limitations

The present study has several limitations that deserve to be mentioned. First, the number of erosions found in the present patient cohort does not correspond to previously reported rates of incidence (22–44%).[2,25] This might be due to the relatively low number of study patients and a selection bias, caused by the entry criteria of the POLARIS-I registry. Second, although we analyzed a substantial number of frames presenting thrombus material, the total number of lesions analyzed was modest and we identified 2 separate thrombus-regions within 5 of the 21 thrombus-containing vessels. We aimed to correct for this by using a nested GLME model. Finally, we assessed the thrombus volume based on images of conventional OFDI intensity. Only clearly identifiable thrombus was delineated, excluding strongly attenuated areas of red thrombus. This may have artificially decreased the depolarization measured in these thrombi, resulting in a similar appearance between all thrombi group; it also impeded us from obtaining the true volume of these thrombi.

Conclusions

In this analysis of the POLARIS-I registry, we were able to demonstrate a significantly higher birefringence in HCTs than in fresh thrombus. Strengthening the latter observation, the ischemic time was a significant predictor of birefringence. These results suggest that birefringence measured with PS-OFDI provides quantitative assessment of coronary thrombus composition and age in vivo. This may enable future research investigating whether the composition of thrombus can help in risk stratification and patient management.

Sources of Funding

Massachusetts General Hospital and the Erasmus University Medical Center have patent licensing arrangements with Terumo Corporation. The Wellman center received institutional support from Terumo Corporation. This work was supported by the National Institutes of Health (grants P41EB-015903 and R01HL-119065) and by Terumo Corporation.

Disclosures

Dr. van Zandvoort received institutional research support from Acist Medical Inc. Dr. Otsuka acknowledges partial support from the Japan Heart Foundation / Bayer Yakuhin Research Grant Abroad, the Uehara Memorial Foundation Postdoctoral Fellowship, and the Japan Society for the Promotion of Science Overseas Research Fellowship. Dr. Bouma was supported, in part, by the Professor Andries Querido visiting professorship of the Erasmus University Medical Center in Rotterdam. Dr. Daemen reports to have received institutional research support from Pie Medical, Acist Medical Inc., PulseCath, Medtronic, Boston Scientific, Abbott Vascular and speaker and consultancy fees from PulseCath, Medtronic, ReCor Medical, Acist Medical Inc.

Drs. Bouma and Villiger have the right to receive royalties as part of the licensing arrangements. All other authors have reported that they have no relationships relevant to the contents of this paper to disclose.

IRB Information

All procedures followed were in accordance with the ethical standards of the responsible committee on human experimentation (institutional and national) and with the Helsinki Declaration of 1975, as revised in 2000. Informed consent for participation in the study was obtained from all patients.

References

1. Falk E. Coronary thrombosis: Pathogenesis and clinical manifestations. *Am J Cardiol* 1991; **68:** 28b–35b.
2. Falk E, Nakano M, Bentzon JF, Finn AV, Virmani R. Update on acute coronary syndromes: The pathologists' view. *Eur Heart J* 2013; **34:** 719–728.
3. Virmani R, Kolodgie FD, Burke AP, Farb A, Schwartz SM. Lessons from sudden coronary death: A comprehensive morphological classification scheme for atherosclerotic lesions. *Arterioscler Thromb Vasc Biol* 2000; **20:** 1262–1275.
4. Claessen BE, Henriques JP, Jaffer FA, Mehran R, Piek JJ, Dangas GD. Stent thrombosis: A clinical perspective. *JACC Cardiovasc Interv* 2014; **7:** 1081–1092.
5. Lee T, Mintz GS, Matsumura M, Zhang W, Cao Y, Usui E, et al. Prevalence, predictors, and clinical presentation of a calcified nodule as assessed by optical coherence tomography. *JACC Cardiovasc Imaging* 2017; **10:** 883–891.
6. Burke AP, Kolodgie FD, Farb A, Weber DK, Malcom GT, Smialek J, et al. Healed plaque ruptures and sudden coronary death: Evidence that subclinical rupture has a role in plaque progression. *Circulation* 2001; **103:** 934–940.
7. Carol A, Bernet M, Curos A, Rodriguez-Leor O, Serra J, Fernandez-Nofrerias E, et al. Thrombus age, clinical presentation, and reperfusion grade in myocardial infarction. *Cardiovasc Pathol* 2014; **23:** 126–130.
8. Rittersma SZ, van der Wal AC, Koch KT, Piek JJ, Henriques JP, Mulder KJ, et al. Plaque instability frequently occurs days or weeks before occlusive coronary thrombosis: A pathological thrombectomy study in primary percutaneous coronary intervention. *Circulation* 2005; **111:** 1160–1165.
9. Silvain J, Collet JP, Nagaswami C, Beygui F, Edmondson KE, Bellemain-Appaix A, et al. Composition of coronary thrombus in acute myocardial infarction. *J Am Coll Cardiol* 2011; **57:** 1359–1367.
10. Kume T, Akasaka T, Kawamoto T, Ogasawara Y, Watanabe N, Toyota E, et al. Assessment of coronary arterial thrombus by optical coherence tomography. *Am J Cardiol* 2006; **97:** 1713–1717.
11. Porto I, Mattesini A, Valente S, Prati F, Crea F, Bolognese L. Optical coherence tomography assessment and quantification of intracoronary thrombus: Status and perspectives. *Cardiovasc Revasc Med* 2015; **16:** 172–178.

12. Tan KT, Lip GY. Red vs white thrombi: Treating the right clot is crucial. *Arch Intern Med* 2003; **163:** 2534–2535.
13. Shimokado A, Matsuo Y, Kubo T, Nishiguchi T, Taruya A, Teraguchi I, et al. In vivo optical coherence tomography imaging and histopathology of healed coronary plaques. *Atherosclerosis* 2018; **275:** 35–42.
14. Villiger M, Otsuka K, Karanasos A, Doradla P, Ren J, Lippok N, et al. Coronary plaque microstructure and composition modify optical polarization: A new endogenous contrast mechanism for optical frequency domain imaging. *JACC Cardiovasc Imaging* 2018; **11:** 1666–1676.
15. Otsuka K, Villiger M, Karanasos A, van Zandvoort LJC, Doradla P, Ren J, et al. Intravascular polarimetry in patients with coronary artery disease. *JACC Cardiovasc Imaging* 2019; **13:** 790–801.
16. Nadkarni SK, Pierce MC, Park BH, de Boer JF, Whittaker P, Bouma BE, et al. Measurement of collagen and smooth muscle cell content in atherosclerotic plaques using polarization-sensitive optical coherence tomography. *J Am Coll Cardiol* 2007; **49:** 1474–1481.
17. Johnson TW, Räber L, di Mario C, Bourantas C, Jia H, Mattesini A, et al. Clinical use of intracoronary imaging. Part 2: Acute coronary syndromes, ambiguous coronary angiography findings, and guiding interventional decision-making: An expert consensus document of the European Association of Percutaneous Cardiovascular Interventions: Endorsed by the Chinese Society of Cardiology, the Hong Kong Society of Transcatheter Endocardiovascular Therapeutics (HKSTENT) and the Cardiac Society of Australia and New Zealand. *Eur Heart J* 2019; **40:** 2566–2584.
18. Villiger M, Zhang EZ, Nadkarni SK, Oh WY, Vakoc BJ, Bouma BE. Spectral binning for mitigation of polarization mode dispersion artifacts in catheter-based optical frequency domain imaging. *Opt Express* 2013; **21:** 16353–16369.
19. Prati F, Guagliumi G, Mintz GS, Costa M, Regar E, Akasaka T, et al. Expert review document part 2: Methodology, terminology and clinical applications of optical coherence tomography for the assessment of interventional procedures. *Eur Heart J* 2012; **33:** 2513–2520.
20. Prati F, Regar E, Mintz GS, Arbustini E, Di Mario C, Jang IK, et al. Expert review document on methodology, terminology, and clinical applications of optical coherence tomography: Physical principles, methodology of image acquisition, and clinical application for assessment of coronary arteries and atherosclerosis. *Eur Heart J* 2010; **31:** 401–415.
21. Mann J, Davies MJ. Mechanisms of progression in native coronary artery disease: Role of healed plaque disruption. *Heart* 1999; **82:** 265–268.
22. Villiger M, Otsuka K, Karanasos A, Doradla P, Ren J, Lippok N, et al. Repeatability assessment of intravascular polarimetry in patients. *IEEE Trans Med Imaging* 2018; **37:** 1618–1625.
23. van der Sijde JN, Karanasos A, Villiger M, Bouma BE, Regar E. First-in-man assessment of plaque rupture by polarization-sensitive optical frequency domain imaging in vivo. *Eur Heart J* 2016; **37:** 1932.
24. Doradla P, Otsuka K, Nadkarni A, Villiger M, Karanasos A, Zandvoort L, et al. Biomechanical stress profiling of coronary atherosclerosis: Identifying a multifactorial metric to evaluate plaque rupture risk. *JACC Cardiovasc Imaging* 2019; **13:** 804–816.
25. White SJ, Newby AC, Johnson TW. Endothelial erosion of plaques as a substrate for coronary thrombosis. *Thromb Haemost* 2016; **115:** 509–519.